Desalination and Water Treatment
www.deswater.com

doi:10.5004/dwt.2018.22450

115 (2018) 135–144
May

Evaluation of batch and continuous adsorption kinetic models of cadmium from aqueous solutions using sugarcane straw nano-structure absorbent

Soheila Farzi[a], Masoumeh Farasati[b,*], Bahman Farhadi Bansouleh[c], Meghdad Pirsaheb[d]

[a]*Department of Water Engineering, Faculty of Agriculture, Razi University, Kermanshah, Iran, Tel. +98 9189918393, email: soheilafarzi@yahoo.com (S. Farzi)*
[b]*Department of Water Engineering, Faculty of Agriculture, Gonbad Kavoos University, Gonbad, Razi University, Kermanshah, Iran, Tel. +98 9188300783, email: Farasati2760@gmail.com (M. Farasati)*
[c]*Department of Water Engineering, Faculty of Agriculture, Razi University, Kermanshah, Iran, Tel. +98 9183587252, email: Bfarhadi2001@yahoo.com (B.F. Bansouleh)*
[d]*Research Center for Environmental Determinants of Health (RCEDH), Kermanshah Medical Sciences, Kermanshah, Iran, email: mpirsaheb@yahoo.com (M. Pirsaheb)*

Received 2 October 2017; Accepted 2 May 2018

ABSTRACT

The purpose of this study was to analyze batch and column adsorption kinetics equations of cadmium from aqueous solutions using sugarcane straw nano-structure absorbent. In the batch experiments, adsorption kinetics was investigated. In the column experiments, a fixed-bed column with 84 cm height (27 cm for free board) and 3.4 cm internal diameter was used. Adsorption column performance for 5, 10 and 20 mg/L cadmium ion, for 0.05 L/min continuous flow rate from up to down and 27 cm bed height was used. Experiments were conducted at the pH = 5 and laboratory temperature condition. Second order kinetics model with $R^2 = 0.974$ and RMSE = 0.002 had the highest correlation with laboratory data. The maximum adsorption capacity of second order kinetics model (1.11 mg/g) was exactly equal to maximum actual adsorption capacity. Continuous test results showed that with increasing concentrations of 5 to 20 mg/L cadmium, the maximum adsorption capacity increased from 0.91 to 2.08 mg/g and the adsorption efficiency decreased from 48.8 to 30.32. The model of Thomas and Yon- Nelson with the correlation coefficient up to 0.95 were more consistent with laboratory data of fixed bed columns compared to Bohart-Adams, and Dose Response models.

Keywords: Sugarcane straw; Cadmium; Continuous and batch system; Kinetic model

1. Introduction

One of the major concerns of developed and developing countries nowadays, is that various water resources are polluted by heavy metals such as cadmium [1]. In many parts of the world, heavy metals, which are found in different physical and chemical forms and at various concentrations, pollute the environment through the discharge of different types of wastewater [2]. Cadmium, as a heavy metal, is not degradable and accumulates in the tissues of living organisms, resulting in kidney disorders and diseases, lung failure, bone defects, and high blood pressure [1,3]. The US Environmental Protection Agency (US EPA) and the International Agency for Research on Cancer (IARC) has recognized cadmium as a carcinogenic substance [4]. Cadmium is used in various industries and products such as batteries, phosphate fertilizers, mines, textiles, and alloys and goes into the environment through the disposal of wastewater produced by these industries [5,6]. Various methods such as chemical precipitation, ion exchange, filtration, reverse osmosis, electro dialysis, and surface adsorption are used to remove heavy metal ions from aqueous media [7]. In

*Corresponding author.

recent years, there has been an increase in the use of surface adsorption which is carried out through the utilization of cheap adsorbent materials obtained from agricultural activities. Because of the presence of compounds such as cellulose, hemi cellulose, lignin, and silica in natural adsorbents and the presence of adsorption sites, they are used as low-cost and green adsorbents [6]. So far, many studies have been conducted to investigate the removal of cadmium using plant adsorbents such as Luffa natural adsorbent [8], orange peel [9], rice ash [10], straw leaf [11], sugarcane bagasse [12], sunflower wastes, canola, and walnut shell [13], olive kernel and sugarcane bagasse [6], sesame waste [14], peanuts shell [15], sweet potatoes [16], and many other things. In order to investigate the removal of heavy metals using adsorbents, adsorption experiments are carried out via two methods including batch and continuous method. In batch experiments, the researchers investigate the ability of the adsorbent material in the adsorption of the desired metal and determine its adsorption capacity in a laboratory scale. Hence, in most cases, the data obtained from these methods cannot be used in an industrial scale. Therefore, it is also necessary to perform continuous experiments in order to obtain data that can be used in an industrial scale [17]. Since heavy metals (including cadmium) are able to reach the aerial parts of plants through irrigation, they are much likely to be used by humans. Moreover, in order to protect plants and water resources, the removal of heavy metals from the environment is very important. The aim of this study was to investigate the kinetics of batch and continuous adsorption of cadmium from aqueous solutions using sugarcane straw nano structure adsorbent. In the batch experiment, we evaluated adsorption kinetics and the step that limits the adsorption rate. In the continuous experiment, we used a fixed-bed column to assess the performance of adsorption column for different concentration of cadmium to the column.

2. Materials and methods

2.1. Preparation of adsorbent

The leaves of sugarcane straw were obtained from the farms owned by Amirkabir Sugarcane Development Company (around Ahwaz). After washing, they were dried in an open place. The dried leaves were milled in a ball mill device for 2 h to change their size into a micrometer size. After the passage of the mentioned time, the obtained particles were passed through sieves with meshes of 20 and 40 to reach a particle size of 420–840 microns. Moreover, after 7 h, the sugarcane straw was converted into a nano structure and using a particle size analyzer the diameters of nano particles were measured.

2.2. Preparation of stock solution

In this research, cadmium nitrate tetrahydrate ($Cd(NO_3)_2{\cdot}4H_2O$) with a concentration of 1000 mg/L was used as the standard solution. The desired solutions were prepared by diluting the standard solution. In different stages of the experiment, the sulfuric acid and 1N NaOH were used to adjust pH value and atomic adsorption spectrophotometer (Model: VARIAN, 220) was used to measure the concentration of the samples.

2.3. Batch experiment study

The kinetic behavior of cadmium ion adsorption on a sugarcane straw nano-structure adsorbent was evaluated via batch experiment at pH = 5 (optimum adsorption pH was obtained from batch experiments). To this end, 30 ml of cadmium nitrate solution was prepared at different concentrations of 5, 10, 15, and 20 mg/L and poured into the containers. Then, 0.5 g of the adsorbent (optimum adsorption mass was obtained from batch experiments) was added to each sample and they were placed on shaker device with a speed of 120 rpm. After the passage of the desired contact times 10, 30, 60, 90, 120, and 360 min, the samples were passed through a filter paper and their concentration was measured using atomic adsorption spectrophotometer.

In order to study the mechanisms controlling the adsorption process, first order kinetics [18], second order kinetics [19], power [20], intra particle diffusion [21], and Elovich models [22] were used. The equation of these models are presented in Table 1. The efficiency and capacity of the adsorption were calculated using Eq. (1) and Eq. (2) respectively.

$$R = \frac{C_i - C_f}{C_i} \times 100 \tag{1}$$

$$q = \frac{C_i - C_f}{M} \times V \tag{2}$$

where R is the adsorption efficiency (%), q is the amount of metal adsorbed to the adsorbent or adsorption capacity (mg/g), V is the volume of solution containing the metal (L), C_i and C_f are initial concentration and equilibrium concentration (mg/L) respectively, and M is the amount of adsorbent (g).

Where k_1 is the rate constant of the pseudo-first-order sorption (g/mg·min), which can be calculated by plotting log ($q_e - q_t$) versus t. k_2 is the rate constant of the pseudo-second order sorption (g/mg·min). α is the Elovich constant which

Table1
Kinetic adsorption models

Kinetic models	Equation
Pseudo-first order kinetic	$q_t = q_e\left(1-\exp\left(-k_1 t\right)\right)$
Pseudo-second order kinetic	$q_t = \frac{K_2 q_e^{\,2} t}{1 + q_e k_2 t}$
Power	$q_t = at^b$
Intra-particle diffusion	$q_t = k_d t^{0.5} + C$
Elovich	$q_t = \frac{1}{\beta} In(\alpha\beta) + \frac{1}{\beta} In(t)$

gives an idea of the reaction rate constant (mg/g/min), β is the Elovich constants and represents the rate of chemisorption at zero coverage (g mg^{-1}), k_d is the intra-particle rate constant (mg/g/$min^{0.5}$), a and b is power constant, q_t is the amount adsorb per gram of sorbent at any time t (mg/g), q_e is the amount adsorb per gram of the sorbent at equilibrium (mg/g), c is the intra particle diffusion constant.

2.4. Desorption experiment

In this step, the adsorbent obtained from batch experiments was first washed by using distilled water and dried in the oven. Then, to investigate the desorption process, 30 ml of 0.1 N hydrochloric acid was added to the optimum amount of the adsorbent (0.5 g) and placed on a shaker with a speed of 150 rpm. After the passage of the desired time, the samples were centrifuged for 15 min with a speed of 2000 rpm and the final concentration of desorption samples was determined. Prior to use in the next round, the used adsorbent in first cycle, was washed again by using distilled water and dried in the oven. The adsorption-desorption process was performed in 5 cycles [1,23].

2.5. Column experiments adsorption

Adsorption in continues adsorption process was carried out using a transparent Plexi glass column with a height of 84 cm, 27 cm as free board, with an internal diameter of 3.4 cm, and an outer diameter of 4 cm. At the end of the column, a filter with 400 micron holes was used for primary filtration of the solution from the adsorbent. From the bottom to the up, it was filled with the coarse sand (more than 0.4 mm thick) and fine sand (0.2–0.4 mm) to a height of 30 cm. We investigated the performance of adsorption column for different concentrations of cadmium metal ion 5, 10, and 20 mg/L, at pH = 5, at a constant flow rate of 0.05 L/min, with a continuous flow from top to bottom, at a bed height of 27 cm, at the laboratory temperature. On the top of the adsorbent, the glass wool was used to smooth the inflow of the solution over the adsorbent surface. The pump used to feed the system was a peristaltic pump, the experiment continue until the time of adsorbent saturation or the experiment continued until the concentration of outlet cadmium reached 95% inlet concentration. Fig. 1 shows a schematic of the continues adsorption process.

Breakthrough time and the shape of the breakthrough curve are the factors that determine the performance and efficiency of an adsorption column [24]. Therefore, to design a column successfully, it is necessary to predict the changes in the concentration of outlet flow with time which is known as the breakthrough curve [25]. In the adsorption process in a fixed bed column, the breakthrough happens when the concentration of the desired ion (Cd(II)) in the outlet flow reaches 3–5% of its concentration in the inlet flow [26]. Moreover, the saturation point is achieved when the ion concentration of ion in the outlet flow reaches a constant value, although the column bed is not completely saturated [27], or when the input and output concentrations are equal [28]. In addition, the saturation point can be achieved when the concentration of the output ion is about 95% of the concentration of input ion [29]. The total amount of adsorbed metal i.e. q_c (mg) for a desired input concentration and flow intensity is equal to the area below the curve of the adsorbed ion concentration ($C_{ads} = C_o - C_e$) over time, and its equation is presented as follows: The total adsorbed metal ion (q_c) by the column can be obtained by integrating the plot of adsorbed cadmium concentration versus the flow time (t). Q is the inlet flow rate to column (ml/min). The area (A) under this integrated plot is substituted in Eq. (3) to determine q_c:

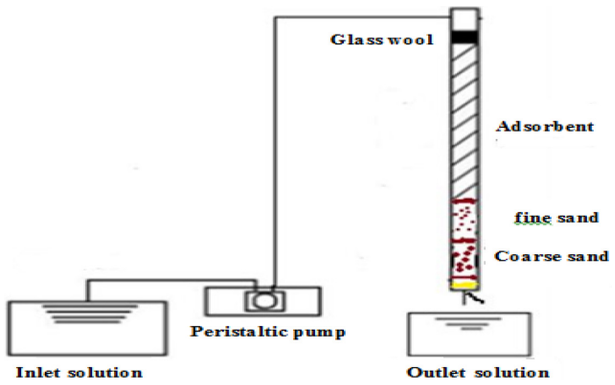

Fig. 1. Schematic of the fixed-bed column.

$$q_c = \frac{QA}{1000} = \frac{Q}{1000}\int_{t=0}^{t=t} C_{ad}\,dt \tag{3}$$

The total amount of metal ions delivered to the column system (m_{total}) is obtained from Eq. (4). The column performance can be evaluated by the total removal percentage of metal ions from the ratio of total adsorbed cadmium to the total amount of input cadmium, as given in Eq. (5).

Adsorption is also a well-known equilibrium separation process for wastewater treatment. Equilibrium studies on adsorption give information about the capacity of the sorbent or the amount required to remove a unit mass of pollutant under the system conditions. As the adsorption isotherms obtained from sorption data in a batch system are not able to represent the column equilibrium, the experimental data from the column experiments should be used to fit isotherm models. Equilibrium cadmium uptake (q_{eq}) (or maximum capacity of the column) in the column is defined by Eq. (6) as the total amount of cadmium sorbed (q_c) per g of sorbent (X) at the end of total flow time [24,30].

$$m_{total} = \frac{C_o \cdot Q \cdot t}{1000} \tag{4}$$

$$R\% = \frac{q_c}{m} * 100 \tag{5}$$

$$q_{\max} = \frac{q_c}{X} \tag{6}$$

2.6. Modeling of continuous experiment data

In order to analyze and explain the laboratory data, four models including Thomas, Bohart-Adams, Yon-Nelson, and Dose Response were used to predict the adsorption process.

2.6.1. Thomas model

The Thomas model is one of the most common and extensively used model to predict the packed bed performance. The Thomas model assumes Langmuir kinetics, no axial dispersion and that the rate driving force obeys second-order reversible reaction kinetics. This model also assumes a constant separation factor which is applicable to either favorable or unfavorable isotherms. The weakness of this model is that its derivation is based on second-order reaction kinetics whereas many times it was found that adsorption is often controlled by inter phase mass transfer. This inconsistency may lead to some error when this method is used to model adsorption process. The breakthrough curves were analyzed by using the Thomas model through the following Eq .(7).

$$\frac{C_t}{C_o}=\frac{1}{1\pm\exp\left(\frac{K_{Th}}{F}\left(q_o m-C_o V_{eff}\right)\right)} \tag{7}$$

The linearized form of the Thomas model can be expressed as follows:

$$In\left(\frac{C_o}{C_t}-1\right)=\frac{K_{Th}q_o m}{F}-K_{Th}C_o t \tag{8}$$

where the kinetic coefficient (K_{Th}) and the maximum biosorption capacity (q_o) can be determined from a plot of $ln[(C_o/C_t) - 1]$ against t at a given flow rate. C_o and C_t are metal ion concentrations (mg L^{-1}) in the influent and effluent, respectively, K_{Th} is the Thomas model rate constant (mL mg^{-1} min^{-1}), F is the flow rate (L h^{-1}), q_o is the maximum solid-phase concentration of the solute (mg g^{-1}), m is the total mass of the biosorbent loaded in the packed bed (g), and V_{eff} is the volume of metal solution passed through the packed bed (L) [29].

2.6.2. Adam- Bohart model

Adam-Bohart model usually used to explain the initial part of breakthrough curves in the adsorption process [31]. One of the most important features of the Adam-Bohart model is its simplicity; it ignores intra-particle diffusion and mass resistance, and the adsorption kinetics are controlled by a surface chemical reaction between the adsorbent and the adsorbed item [27].

$$\frac{C}{C_o}=\frac{e^{r}}{e^{r}+e^{\xi}-1} \tag{9}$$

$$\tau=kC_o\left(t-\frac{z}{\nu}\right) \tag{10}$$

$$\xi=\frac{kq_s z}{\nu}\left(\frac{1-\varepsilon}{\varepsilon}\right) \tag{11}$$

The transformed variables τ and ξ are, respectively, a dimensionless time and distance. The exit concentration is obtained by setting z = L , where L is the length of the bed. The use of the Bohart-Adams model to design adsorbent beds requires accurate knowledge of the two parameters k and q_s. These parameters are not easily predicted since they represent the aggregate effects of mass transfer, pore diffusion, kinetics of adsorption and equilibrium. It is custom to rewrite Eq. (9) to facilitate the fit to the breakthrough data. The reciprocal of Eq. (9), after some trivial algebra, can be written as:

$$\frac{C}{C_o}-1=e^{\xi-t}-e^{-t} \tag{12}$$

The second term on the right side is usually small and can be neglected. We also recognize that for long times, the term z/ν in the expression for τ can be ignored. Taking natural logarithms yields the equation:

$$In\left(\frac{C_t}{C_o}\right)=K_{BA}C_o t-\frac{K_{AB}N_o Z}{U_o} \tag{13}$$

The k_{AB} in this equation represents the Adam-Bohart kinetic constant (L/mg min), The N_o and Z are the saturation concentration (mg/L) and the bed depth of column (cm), respectively. The U_o represents the linear velocity (cm/min) determined from the calculation of volumetric flow rate over the bed section area. The value of k_{AB} and N_o can be obtained from the plot of $ln\ (C_t/C_o)$ versus t [31].

2.6.3. Yoon–Nelson model

This model is based on assumption of the probability of adsorbate adsorption and breakthrough. The Yoon and Nelson model not only is less complicated than other models, but also requires no detailed data regarding the characteristics of adsorbate, the type of adsorbent, and the physical properties of the bed. The Yoon and Nelson equation regarding to a single component system is expressed as:

$$In\left(\frac{C_t}{C_o}\right)=\frac{\exp\left(K_{YN}t-\tau K_{YN}\right)}{1\pm\exp\left(K_{YN}t-\tau K_{YN}\right)} \tag{14}$$

The linear form of Yoon–Nelson model can be expressed as:

$$In\left(\frac{C_t}{C_o-C_t}\right)=K_{YN}t-\tau K_{YN} \tag{15}$$

The k_{YN} and τ in this equation represent the Yoon–Nelson rate of constant (min^{-1}) and time required for 50% of adsorbate break-through (min). Other physical column parameters are not required for this model equation. The value of k_{YN} and τ can be obtained from the plot of *ln (Ct/(Co – Ct)) vs. t* (29).

2.6.4. Dose response model

This model was initially developed for pharmacology studies and recently used to describe adsorption of metals in some cases. The modified dose-response model can be written as:

$$\frac{C}{C_F}=1-\frac{1}{1+\left(\frac{C_F Qt}{q_F m}\right)^{a}} \tag{16}$$

After rearrangement, it could be written as:

$$In\left(\frac{C}{C_F - C}\right) = aLn\left(C_F Qt\right) - aLn\left(q_F M\right) \quad (17)$$

where a is the model parameter. Similar to other models, a and q_F could be determined by plotting $ln[C/(C_F - C)]$ vs. ln $(C_F Q_t)$. Where C_F and C is inlet and outlet concentration in zero time (mg/l), t is the time (min), Q is the inlet flow rate (lit/min), m is the adsorbent mass in column (g), q_f is the adsorptive capacity (mg/g), a is the empirical parameters [32].

In order to evaluate the models we used the coefficient of determination R^2 and root-mean-square error (RMSE).

$$RMSE = \sqrt{\frac{\sum_{i=1}^{n}\left(qe - qc\right)^2}{n}} \quad (18)$$

where q_e calculated adsorption capacity from experiment (mg/g), q_c adsorption capacity calculated by model (mg/g), n is the number of measured data.

3. Result and discussion

3.1. Results of absorbent properties

The results of particle size analysis of nano-structure sugarcane straw adsorbent are presented in Fig. 2. As shown the curve of particle size analysis of sugarcane straw has a normal distribution and all particles had a diameter less than 327.5 nm and are converted into nano-structures.

3.2. Batch kinetic studies

Fig. 3 shows the variations in initial concentration with time and its effect on the adsorption efficiency. As shown in Fig. 3, with increasing the initial concentration of cadmium, the percentage of adsorption efficiency decreased. We also tested the effect of initial concentration on the adsorption efficiency; since the amount of adsorbent is constant, there were many adsorption sites at low concentration levels and therefore, cadmium ions were easily adsorbed. In fact, with increasing the cadmium concentration, the amount of adsorption increases, however, because of the constant adsorbent ratio, the adsorption efficiency decreases due to the saturation of adsorption sites [8,33,34].

Table 2 shows the results of the fitting of adsorption kinetics models on the adsorption of cadmium ions by the sugarcane straw nano-structure adsorbent. The results of the kinetic models are presented in Table 2, as shown, the second order kinetics model with $R^2 = 0.974$ and RMSE = 0.002 had the largest level of agreement with the experimental data. The amount of adsorption capacity calculated by the first-order kinetic model (1.01 mg/g) was lower than the actual adsorption capacity (1.11 mg/g), and the adsorption capacity calculated by the second order kinetic model (11.1 mg/g) was exactly equal to the actual adsorption capacity. In the intra-particle diffusion model, the obtained equation had a non-zero intercept, which showed that intra-particle diffusion alone was not able to control the adsorption rate.

3.3. Desorption result

We investigated the adsorption-desorption cycles using hydrochloric acid and the results showed that after 5 times of washing and removal of cadmium ions from adsorbent by using hydrochloric acid, adsorption efficiency was still higher than 75%. Therefore, it can be said that the adsorption of cadmium ions on the sugarcane straw absorbent was a physical mechanism. Thus, this adsorbent can be used as a recyclable absorbent for the removal of cadmium, which is both economically and environmentally useful and acceptable.

3.4. Study of column adsorption

Table 3 presents the performance of column adsorption for different input concentrations of cadmium ions 5, 10, and

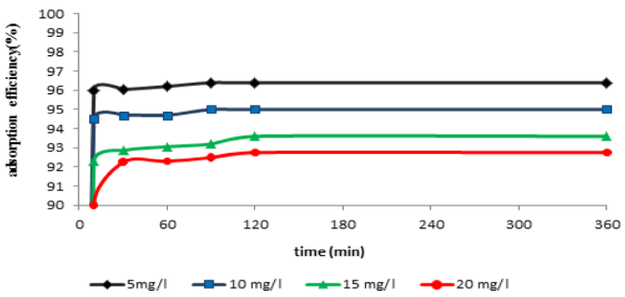

Fig. 3. Initial concentration changes with time and its effect on adsorption efficiency (Adsorbent 0.5 g in 30 ml solution, pH = 5).

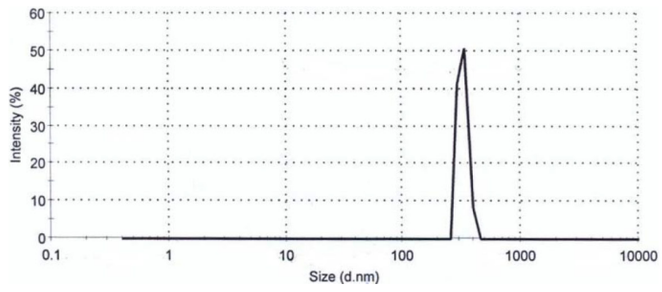

	Diam. (nm)	% Intensity	Width (nm)
Peak 1:	327.5	100.0	30.50
Peak 2:	0.000	0.0	0.000
Peak 3:	0.000	0.0	0.000

Fig. 2. Particles size distribution of nano structure of sugarcane straw adsorbent.

Table 2
Kinetic parameters for the adsorption of Cd^{2+} onto nano structure of sugar cane straw (Adsorbent 0.5 g in 30 ml solution, pH = 5, cadmium concentration 20 mg/L)

Model	Parameter			
Pseudo-first order kinetic	K_1 (min^{-1})	q_e (mg g^{-1})	R^2	RMSE
	0.00005	1.01	0.271	1.09
Pseudo- second order kinetic	K_2 (g mg^{-1} min^{-1})	k (g mg^{-1} min^{-1})	R^2	RMSE
	3.53	1.11	0.974	0.002
Power	A	B	R^2	RMSE
	1.07	0.008	0.710	0.006
Intra-particle diffusion	k_i (g mg^{-1} min^{-1})	C	R^2	RMSE
	0.001	1.09	0.746	0.008
Elovich	α	β	R^2	RMSE
	0.04	114.94	0.714	1.055

Table 3
Breakthrough curve parameters of Cd^{+2} adsorption for varying initial concentration

C_0 (mg/l)	t_b (min)	$\tau_{50\%(YN)}$	t_e (min)	q_c (mg)	m_{total} (mg)	R%	q_{max} (mg/g)
5	81.8	250.6	350.8	43.9	90	48.8	0.91
10	51	205	285.4	65.6	180	36.45	1.36
20	14.3	167.5	254.2	100	330	30.32	2.08

20 mg/L at a flow rate of 0.05 L/min and a bed height of 27 cm. The results showed that with increasing the concentration of cadmium ion inflow to the column from 5 to 20 mg/L, the parameters of time breakthrough, the time required for achieving 50% of the adsorption curve (the time when the outflow concentration is half of inflow concentration), and the time of column saturation, respectively, changed from 81.8, 250.6, and 350.8 min to 14.3, 167.5, and 254.2 min, because with increasing the concentration, the adsorbent particles was contacted to high concentrations of cadmium ions, which resulted in a faster saturation of the adsorption column. With increasing the inlet concentration to the column from 5 to 20 mg/L, the maximum adsorption capacity changed from 0.91 to 2.08 mg/g, but the adsorption efficiency decreased from 48.8% to 30.32%. With increasing the concentration of inflow cadmium ion, there was an increase in the adsorption capacity which might be attributed to the increase in mass transfer between the adsorbent and the fluid, or the driving force of the mass transfer in the adsorption process that overcomes the resistance to mass transfer. Therefore, the mass transfer rate and, consequently, the adsorption capacity are increased. In fact, the increase in the concentration of inflow ion provides condition for increasing the driving force and thus increases the chemical adsorption potential [14,24,31,35]. With increasing the concentration of inflow ion to the column there was a decrease in the percentage of adsorption efficiency which might also be due to the saturation of the adsorbent mass loaded in the adsorption column [14].

Where C_0 is influent cadmium concentration, t_b is breakthrough time, $t_{50\%}$ is the required time for achieving 50% of the breakthrough curve, t_e time of saturation, q_c total cadmium uptake (mg), m_{total} total inlet ion concentration, R adsorption efficiency, q_{max} maximum adsorption capacity of column(mg/g).

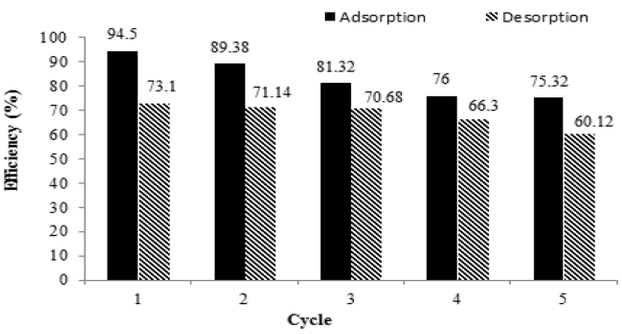

Fig. 4. Adsorption–desorption efficiency in adsorption-desorption cycles.

Fig. 5 confirms the above mentioned results and shows that in lower inflow concentrations, the breakthrough curves are longer with a softer slope; in addition, the saturation point is achieved over a longer period of time. This process indicates that the mass transfer region was relatively broad, and there was thin layer of fluid surrounding the adsorbent that has controlled the process of adsorption. However, with the increase in the concentration of the ion inflow to the column, the slope of the breakthrough curves had become steeper and the column reached the saturation point more quickly; this phenomenon is attributed to the small size of the mass transfer area and the infiltration of material into the pores of the adsorbent [36,37]. The increase in the driving force is a factor involved in increasing the adsorption capacity in continuous experiments [8,35,38]. Similar results have been achieved by other researchers [39,40].

The highest adsorption efficiency of cadmium in a fixed bed column at pH = 5, a concentration of 5 mg/L, a flow rate of 0.05 L/min, and a bed depth of 27 cm away from the adsorbent was 48.8%.

3.5. Assessment of breakthrough curves

Table 4 presents the results of the evaluation of dynamic behavior of cadmium adsorption by the sugarcane straw nano structures which were calculated by using the Thomas, Adam-Bohart, Yon-Nelson, and dose response models. The results of fitting the Thomas model showed that the maximum adsorption capacity (q_{Th}) and the Thomas velocity constant (k_{Th}) with increasing the concentration of cadmium ion inflow to the column were increased and decreased, respectively. It is consistent with the results of the previous studies [14,24,37,40]. In fact, with increasing the concentration of ion inflow to the column and consequently increasing the driving force and chemical potential, the adsorption process has become more favorable and the adsorption capacity increases [31]. Comparing the maximum adsorption capacity obtained from the model and the laboratory data available in Tables 3 and 4, it is observed that the maximum adsorption capacity estimated by the Thomas model was higher than the actual value for all the concentrations. Considering a correlation coefficient more than 0.95, they were well fitted to the laboratory data; this good fitting might be attributed to the fact that based on Thomas's assumptions, the adsorption rate is controlled by the surface reaction between adsorbed material and adsorbent which control the empty capacities of the adsorbent. Thus, the internal and external diffusion and the resulting resistance are not among the factors that limit the rate of adsorption [14,24,40,41]. On the other hand, Thomas's model assumes that the kinetic of the reaction is a second-order kinetic which is consistent with the results of the fitting of kinetic models in batch experiments. In the Adam-Bohart model, with increasing cadmium concentration, saturation concentration (N_o) and Bohart-Adams kinetic constant (K_{AB}) increased and decreased, respectively. In addition, in the Yon-nelson model, with increasing cadmium concentration inflow, the fixed column rate and the required time for achieving 50% of the breakthrough curve decreased. In fact, with increasing the concentration from 5 to 20 mg/L, the time required for achieving 50% of the adsorption curve decreased from 250.6 to 167.5 min, which is consistent with the results of Rao's study [40]. The results of the fitting of the dose response model showed that with increasing the concentration, the adsorption capacity increased too. Table 4. show the results of the comparison between the maximum adsorption capacity of the dose response and Thomas models. As shown the maximum adsorption capacities obtained from the two models are approximately the same and both models estimated values which were more than the actual value.

Figs. 6a, b, c, d show the fitting of continuous adsorption models on experimental data at various concentrations (5, 10, and 20 mg/l).

The results showed that the two models i.e. Thomas and Yon-Nelson model which had a correlation coefficient greater than 0.95 for all the concentrations had the highest level of consistency with the experimental data. Comparing the equations of Thomas and Yon-Nelson model, it is observed that although these two models differ in terms of their defined coefficients, the overall shape of the breakthrough curves and the values of coefficients of determination obtained for all concentrations are similar; therefore, it is expected that these two models provide a similar estimate of the maximum adsorption capacity. Other researchers who fitted the Thomas and Yon-Nelson model on the data obtained from the adsorption column also achieved the same results [14,35].

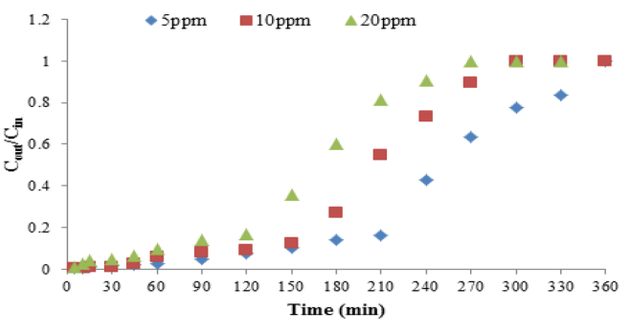

Fig. 5. The effect of initial concentration of Cd^{+2} on Breakthrough curve.

6. Conclusion

We also fitted the results of the batch kinetics adsorption models on laboratory data, and the results showed that the second order kinetics model with $R^2 = 0.974$ and RMSE = 0.002 had the highest levels of consistency with the experimental data. The results of the evaluation of adsorption column performance for different concentrations of cadmium ion inflow to the column with a steady flow showed that with increasing the concentrations, the rate of loading cadmium ion on the bed increases and the driving force of the mass transfer increases too. It also shortens the length

Table 4
Result of adsorption column models

Condition	Thomas			Adam-Bohart				Yon- Nelson			Dose response		
C_i	K_{Th}	q_{Th}	R^2	U	K_{BA}	N_0	R^2	K_{YN}	$\tau_{50\%(YN)}$	R^2	a	q_F	R^2
5	3.72	1.4	0.987	5.5	0.003	324.96	0.863	0.018	271	0.987	1.632	1.76	0.854
10	1.76	2.7	0.958	5.5	0.001	597.03	0.845	0.017	259.5	0.958	1.639	2.87	0.912
20	0.76	4.6	0.956	5.5	0.0006	1086.1	0.932	0.015	221.2	0.956	1.358	4.18	0.911

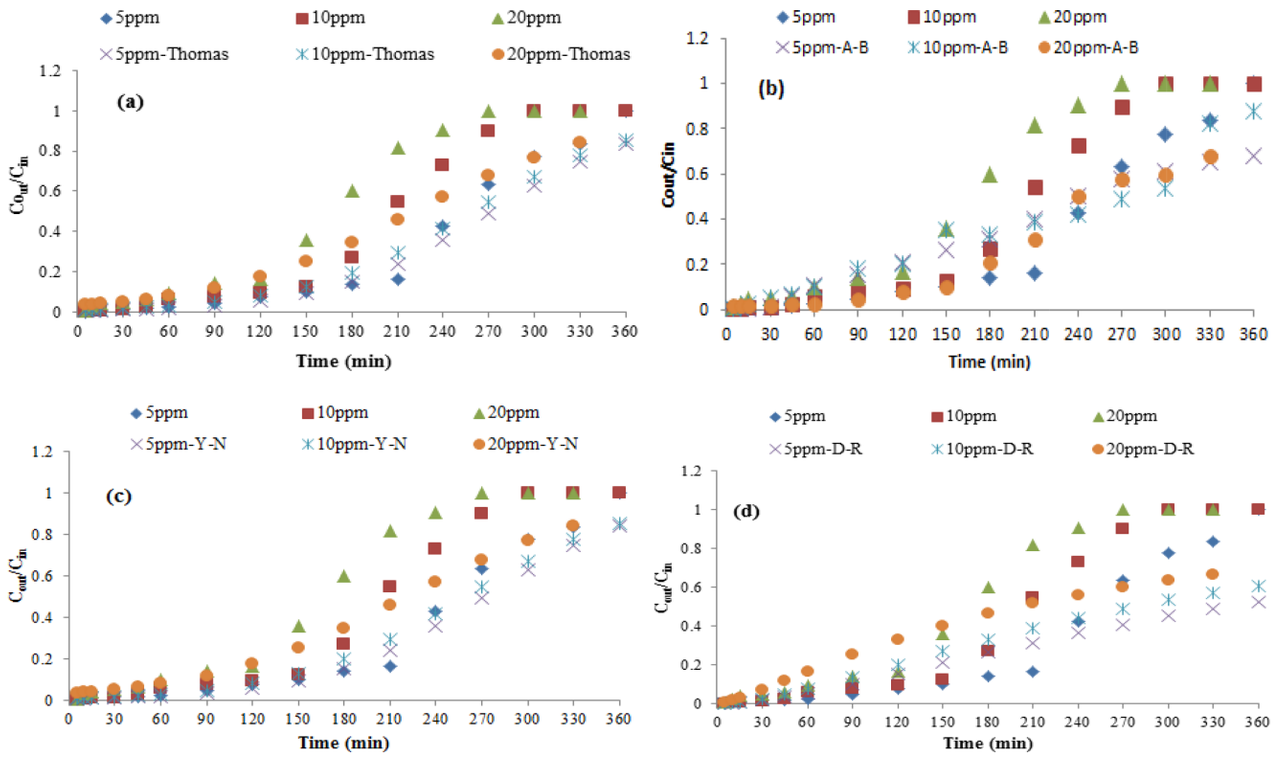

Fig. 6. (a), (b), (c) & (d) are Cd(II) removal predicted by the Thomas model Adam-Bohart, Yoon–Nelson model and dose response model respectively.

of the mass transfer region, thus the column is saturated more quickly. With increasing the concentration from 5 to 20 mg/L, the maximum adsorption capacity increased from 0.91 to 2.08 mg/g, and the adsorption efficiency changed from 48.8% to 30.32%. The highest removal rate of cadmium in the fixed bed column with a pH = 5, concentration of 5 mg/L, and flow rate of 0.05 L/min, and bed depth of 27 cm from the adsorbent was 48.8%. Thomas and Yon-Nelson models with a coefficient of determination higher than 0.95 for all the concentrations were in a good agreement with experimental results. Moreover, the results of desorption showed that the mechanism of adsorption of cadmium ions on the adsorbent is a physical mechanism and it can be used as a recyclable absorbent.

Symbols

A — The area under integrated plot
a, b — Power constant
C_{ad} — Adsorbed cadmium concentration in the column (mg L^{-1})
C_0, C_t — Metal ion concentrations in the influent and effluent, respectively (mg L^{-1})
C_i,C_f — Initial and equilibrium concentration respectively (mg/L)
K_1 — Rate constant of the pseudo-first-order sorption (g/mg·min)
K_2 — Rate constant of the pseudo-second order sorption (g/mg·min)
K_{AB} — Adam- Bohart kinetic constant (L/mg min)
K_d — Intra-particle rate constant (mg/g/$min^{0.5}$)
K_{Th} — Thomas model rate constant (mL mg^{-1} min^{-1})
K_{YN} — Yoon–Nelson rate of constant (min^{-1})
M — Weight of dried adsorbent added to the solution (g)
m_{total} — Total amount of metal ions delivered to the column system (g)
N_0 — Saturation concentration (mg/L)
q_e — Amount adsorb per gram of the sorbent at equilibrium (mg/g)
Q — Inlet flow rate to column (ml/min)
q_c — Total adsorbed metal ion (mg)
q_F — Maximum adsorption capacity in Dose Response model (mg/g)
q_{max} — Maximum adsorption capacity of column (mg/g).
q_t — Amount adsorb per gram of sorbent at any time (mg/g)
q_{Th} — Maximum adsorption capacity in Thomas model (mg/g)
R — Adsorption efficiency (%)
R^2 — Coefficient of determination
RMSE — Root-mean-square error
t_b — Breakthrough time (min)
t_b — Saturation time (min)
$t_{50\%}$ — Require time for achieving 50% of the breakthrough curve (min)
U_0 — Linear velocity (cm/min)
V — Volume of solution containing the metal (L)

V_{eff} — Volume of metal solution passed through the packed bed (L)
X — Unit mass of adsorbent packed in the column (g)
Z — Depth of column (cm)
α,β — Elovich constant (mg/g/min) and (g mg^{-1}) respectively

References

[1] P. Chand, A. Bafana, Y.B. Pakade, Xanthate modified apple pomace as an adsorbent for removal of Cd (II), Ni (II) Pb (II), and its application to real industrial wastewater, Inter. Biodet. Biodeg., 97 (2015) 60–66.
[2] S.K.R. Yadanaparthi, D. Graybill, R. von Wruszka, Adsorbents for the removal of arsenic, cadmium, lead from contaminated waters, J. Hazard. Mater., 171 (2009) 1–15.
[3] M.P. Waalkes, Cadmium carcino genesis in review, J. Inorg. Biochem., 79 (2000) 241–244.
[4] WHO, Air quality guidelines for europe, 2nd ed., WHO Regional Publications, (2006).
[5] V.K. Gupta, C. Jain, I. Ali, M. Sharma, V. Saini, Removal of cadmium nickel from wastewater using bagasse fly ash a sugar industry waste, Water Res., 37 (2003) 4038–4044.
[6] A. Moubarik, N. Grimi, Valorization of olive stone sugar cane bagasse by-products as biosorbents for the removal of cadmium from aqueous solution, Food Res. Inter., 73 (2015) 169–175.
[7] F. Ghorbani, H. Younesi, S.M. Ghasempouri, A.A. Zinatizadeh, M. Amini, A. Daneshi, Application of response surface methodology for optimization of cadmium biosorption in an aqueous solution by Saccharomyces cerevisiae, Chem. Eng. J., 145 (2008) 267–275.
[8] A. Shahidi, N.J. Fallizi, A.J. Fallizi, Evaluation of the natural adsorbent luffa cylindrical for the removal of cadmium (II) from aqueous environments, J. Water Wastewater., 3 (2015) 51–61. (in Persian)
[9] V.K. Gupta, A. Nayak, Cadmium removal recovery from aqueous solutions by novel adsorbents prepared from orange peel Fe_2O_3 nano particles, Chem. Eng. J., 180 (2012) 81–90.
[10] H.A. Hegazi, Removal of heavy metals from wastewater using agricultural industrial wastes as adsorbents, J. HBRC., 9 (2013) 276–282.
[11] T.G. Ammari, Utilization of a natural ecosystem bio-waste; leaves of Arundo donax reed, as a raw material of low-cost eco-biosorbent for cadmium removal from aqueous phase, Ecolo. Eng., 71 (2014) 466–473.
[12] X. Niu, L. Zheng. J. Zhou, Z. Dang, Z. Li, Synthesis of an adsorbent from sugarcane bagass by graft copolymerization its utilization to remove Cd (II) ions from aqueous solution, J. Ins. Chem. Eng., 45 (2014) 2557–2564.
[13] M. Feizi, M. Jalali, Removal of heavy metals from aqueous solutions using sunflower, potato, canola walnut shell residues, J. Ins. Chem. Eng., 54 (2015) 125–136.
[14] E. Cheraghi, E. Ameri, A. Moheb, Continuous biosorption of Cd (II) ions from aqueous solutions by sesame waste: thermodynamics fixed-bed column studies, Desal. Water Treat., 57 (2015) 1–14.
[15] Q. Cheng, Q. Huang, S. Khan, Y. Liu, Z. Liao, G. Li, Y.S. Ok, Adsorption of Cd by peanut husks peanut husk biochar from aqueous solutions, Ecol. Eng., 87 (2016) 240–245.
[16] E.D. Asuquo, A.D. Martin, Sorption of cadmium (II) ion from aqueous solution onto sweet potato (Ipomoea batatas L.) peel adsorbent: Characterisation, kinetic isotherm studies, J. Environ. Chem. Eng. J., 4 (2016) 4207–4228.
[17] M.M. Sekhula, J.O. Okonkwo, C.M. Zvinowa, N.N. Agyei, A.J. Chaudhary, Fixed bed column adsorption of Cu (II) onto maize tassel-PVA beads, J. Chem. Eng. Process Technol., 3 (2012).
[18] R. Malekian, J. Abedi-Koupai, S.S. Eslamian, S.F. Mousavi, K.C. Abbaspour, M. Afyuni, Ion-exchange process for ammonium removal release using natural Iranian zeolite, Appl. Clay Sci., 51 (2011) 323–329.
[19] M. Ghasemi, M. Naushad, N. Ghasemi, Y. Khosravi-fard, Adsorption of Pb (II) from aqueous solution using new adsorbents prepared from agricultural waste: Adsorption isotherm kinetic studies, J. Ind, Eng. Chem., 20 (2014) 2193–2199.
[20] M. Shirvani, H. Shariatmadari, M. Kalbasi, Kinetics of cadmium desorption from fibrous silicate clay minerals: Influence of organic ligs aging, Appl. Clay Sci., 37 (2007) 175–184.
[21] M. Abedi, M.H. Salmani, S.A. Mozaffari, Adsorption of Cd ions from aqueous solutions by iron modified pomegranate peel carbons: kinetic and thermodynamic studies, Int. J. Environ. Sci. Technol., 13 (2016) 2045–2056.
[22] M. Ossman, M. Mansour, M. Fattah, N. Taha, Y. Kiros, Peanuts shell talc powder for removal of hexavalent chromium from aqueous solutions, Bulg. Chem. Comm., 3 (2014) 629–639.
[23] M. El-Sadaawy, O. Abdelwahab, Adsorptive removal of nickel from aqueous solutions by activated carbons from doum seed (Hyphaenethebaica) coat, Alexria Eng. J., 53 (2014) 399–408.
[24] B.S. Smolyakov, A.K. Sagidullin, A.L. Bychkov, I.O. Lomovsky O.I. Lomovsky, Humic-modified natural and synthetic carbon adsorbents for the removal of Cd (II) from aqueous solutions, J. Environ. Chem. Eng., 3 (2015) 1939–1946.
[25] Z. Aksu, F. Gönen, Biosorption of phenol by immobilized activated sludge in a continuous packed bed: prediction of breakthrough curves, Process Biochem., 39 (2004) 599–613.
[26] G. Yan, T. Viraraghavan, Heavy metal removal in a biosorption column by immobilized M. rouxii biomass, Bioresour. Technol., 78 (2001) 243–249.
[27] J.P. Chen, J.T. Yoon, S. Yiacoumi, Effects of chemical physical properties of influent on copper sorption onto activated carbon fixed-bed columns, Carbon, 41 (2003) 1635–1644.
[28] P. Lodeiro, R. Herrero, M.S. De Vicente, Batch desorption studies multiple sorption–regeneration cycles in a fixed-bed column for Cd (II) elimination by protonated Sargassum muticum, J. Hazard. Mater., 137 (2006) 1649–1655.
[29] B.Y. Chen, C.Y. Chen, W.Q. Guo, H.W. Chang, W.M. Chen, D.J. Lee, J.S. Chang, Fixed-bed biosorption of cadmium using immobilized Scenedesmus obliquus CNW-N cells on loofa (Luffa cylindrica) sponge, Bioresour. Technol., 160 (2014) 175–181.
[30] S. Pilli, V.V. Goud, K. Mohanty, Biosorption of Cr (VI) on immobilized Hydrilla verticillata in a continuous up-flow packed bed: prediction of kinetic parameters breakthrough curves, Desal. Water Treat., 50 (2012) 115–124.
[31] J. Cruz-Olivares, C. Perez-Alonso, C. Barrera-Diaz, F. Ureña-Nuñez, M.C. Chaparro-Mercad, B. Bilyeu, Modeling of lead (II) biosorption by residue of allspice in a fixed-bed column, Chem. Eng. J., 228 (2013) 21–27.
[32] A.P. Lim, A.Z. Aris, Continuous fixed-bed column study adsorption modeling: Removal of cadmium (II) lead (II) ions in aqueous solution by dead calcareous skeletons, BioChem. Eng. J., 87 (2014) 50–61.
[33] Z. Xu, J.g. Cai, B.c. Pan, Mathematically modeling fixed-bed adsorption in aqueous systems, J. Zhejiang University Sci. Appl. Phys. Eng., 14 (2013) 155–176.
[34] F.H. Motamedi, N. Mouazed, A.J. Haghighifard, M. Amiri, Investigation of kinetics and isotherms of cadmium adsorption from aqueous solutions using nanoclay, J. Water Waste., 3 (2014) 118–126. (in Persian)
[35] F.Y. Wang, H. Wang, J.W. Ma, Adsorption of cadmium (II) ions from aqueous solution by a new low-cost adsorbent bamboo charcoal, J. Hazard. Mater., 177 (2010) 300–306.
[36] A. Keshtkar, H. Dastehbashi, M.G. Turkabad, M.A. Mousavi, Investigating the effect of concentration and inflow rate of fixed-bed column on the bio-adsorption of nickel by Cystoseira indica-induced brown algae and modeling the experimental results, Ir. J. Health. Environ., 6 (2013) 417–430. (in Persian)
[37] M. Shamsuddin, M.N. Zarandi, M. Fazli, K.L. Haghbin, Removal of strontium (II) from aqueous solutions through adsorption surface method by exogel derived from TEOS: A review of a batch system and fixed bed column, Sci. Res. J. Appl. Chem., 9 (2014) 35–50. (in Persian)

[38] S.S. Baral, N. Das, T.S. Ramulu, S.K. Sahoo, S.N. Das, G.R. Chaudhury, Removal of Cr(VI) by thermally activated weed Salvinia cucullata in a fixed-bed column, J. Hazard. Mater., 161 (2009) 1427–1435.
[39] M. Farasati, Evaluation of the Effects of straw and sugarcane straw nano-structure on nitrate removal from contaminated water, PhD thesis. Irrigation and Drainage. Shahid Chamran Uni, Ahwaz., 2011. (in Persian)
[40] M.H. Ehrampoush, H. Masoudi, A.H. Mahvi, M.H. Salmani, Prevalent kinetic model for Cd (II) adsorption from aqueous solution on barley straw, Fresenius Environ. Bull., 22 (2013) 2314–2318.
[41] K.S. Rao, S. Anand, P. Venkateswarlu, Modeling the kinetics of Cd (II) adsorption on Syzygium cumini L leaf powder in a fixed bed mini column, J. Ind. Eng. Chem., 17 (2011) 174–181.
[42] J. Nwabanne, P. Igbokwe, Adsorption performance of packed bed column for the removal of lead (II) using oil palm fiber, Inter. J. Appl. Sci. Technol., 2 (2012) 106–115.